≪Research Paper≫ Applied Science and Convergence Technology Vol.23 No.1, January 2014, pp.48~53
http://dx.doi.org/10.5757/ASCT.2014.23.1.48

Facile Preparation of Pyrene-templated Hexagonal-shaped Gold Nanoplates

Eun-Kyung Lim[a,b,c], Eunji Jang[d], Seungjoo Haam[b,d], and Yong-Min Huh[a,b]*

[a]*Department of Radiology, Yonsei University, Seoul 120-752*
[b]*YUHS-KRIBB Medical Convergence Research Institute, Seoul 120-752*
[c]*BioNanotechnology Research Center, Korea Research Institute of Bioscience and Biotechnology, Daejeon 305-806*
[d]*Department of Chemical and Biomolecular Engineering, Yonsei University, Seoul 120-749*

(Received January 7, 2014, Revised January 21, 2014, Accepted January 21, 2014)

We have formulated hexagonal-shaped gold nanoplates in a single-step for photothermal therapy that gold ions to gold particles using pyrenyl dextran as reducible stabilizer and template. They exhibit anisotropic structure with broad surface plasmon resonance (SPR) band into near-infrared (NIR) spectrum enabling photothermal therapy. These gold nanoplates are also confirmed biocompatibility and high uptake efficiency due to binding with dextran molecules on the surface of gold nanoplates and cells. From *in vitro* phtothermal ablation study under NIR laser, gold nanoplates have the potential to use as photothermal agents.

Keywords : Gold nanoparticle, Photothermal therapy, Hexagonal-shaped, Near-infrared Absorption, Surface plasmon resonance

I. Introduction

Gold nanoparticles have attracted considerable attention because of their interesting physicochemical properties controllable depending on their size, shape, surfaces and interfacial structures [1,2]. Especially, anisotropic gold nanostructures are an interesting class of structures due to their unique optical, electrical, magnetic and catalytic properties that directly correlate with their shape and size [3-6]. They have been synthesized using a variety of methods, including chemical reduction and seed- mediated growth methods in aqueous phase [7]. Gold salts ($HAuCl_4$) are reduced to gold particles using citrated as a reducing and capping agent, which is well-known as Turkevich method, as the simplest and most commonly ways [8,9]. The size and morphology of gold particles could be controlled by capping agents as template because these agents for an organic matrix exerted an influence on the specific interactions between organic molecules and inorganic materials. These template-mediated syntheses are the most effective approaches for anisotropic structure [10-22].

Recently, it has been reported the synthesis of graphene-gold nanostructures by directly reducing gold precursor in the presence of graphene oxide sheets, which is the oxidized graphene with abundant oxygen functional groups (e.g., - OH, -COOH, epoxy) with a single layer of carbon atoms arranged in the honey comb lattice as template, without any sta-

* [E-mail] ekekek1112@daum.net

bilizers or reducing agents [23-25]. In addition, we confirmed the synthesis of gold nanoparticles using pyrenyl dextran as a reducible stabilizer in previous our report [26]. Herein, we attempted to formulate gold nanoplates of hexagonal shapes using pyrenyl dextran as reducible stabilizer in a single-step by adjusting the ratio between gold ions and pyrenyl dextran because pyrenyl dextran has abundant carbon atoms of pyrenyl groups and oxygen functional groups in dextran as graphene oxide [Fig. 1(a)].

II. Materials and Methods

1. Materials

1-Pyrenebutyric acid, 1,3-dicyclohexylcarbodiimide (DCC), 4-dimethylaminopyridine (DMAP), anhydrous dimethyl sulfoxide (DMSO), triethylamine (TEA), and gold (III) chloride trihydrate ($HAuCl_4$) were purchased from Sigma Aldrich. Dextran T-10 (MW: 10,000 Da) and the dialysis membrane (MWCO: 3500) were obtained from Pharmacia Biotech and Pierce, respectively.

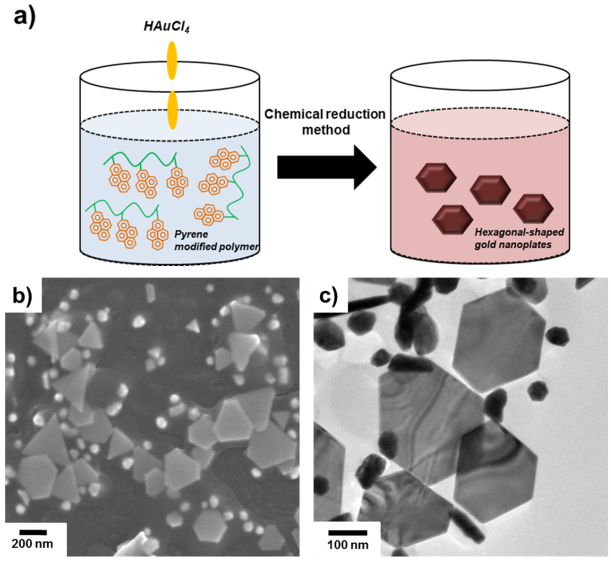

Figure 1. (a) Illustration of experimental procedure for hexagonal-shaped gold nanoplates, (b) SEM and (c) TEM image of hexagonal-shaped gold nanoplates.

2. Synthesis of pyrene modified polymer

We synthesized pyrene modified polymer by conjugating 1-pyrenebutyric acid (Mw: 288.64 Da) and dextran using DCC and DMAP and also confirmed their characteristics, as previously reported [26].

3. Preparation of hexagonal shaped – gold nanoplates

For preparation of gold nanoplates, 200 mg of pyrene modified polymer dissolved in 100 mL of deionized water under vigorous stirring at 95°C, and then 1 mL of a 1 wt % $HAuCl_4$ solution was quickly injected and the solution was kept under stirring at 95°C until the color of the solution changed from light yellow to deep reddish brown [26]. This solution was cooled naturally to room temperature and excess polymer was removed by centrifugation. The morphology of gold nanoplates were observed using scanning electron microscopy (SEM, JSM-6701F, JEOL), transmission electron microscopy (TEM, JEM-1011, JEOL) at an acceleration voltage of 80kV, High-resolution TEM, and energy-dispersive X-ray spectroscopy (EDS) studies (TECNAI G2 F30) operated at 300 kV. The UV-Vis absorbance spectrum and crystallinities of gold nanoplates was measured using an Optizen UV-Vis spectrometer (2120UV; Mecasys, Korea) and X-ray diffraction (Rigaku, X-ray Diffractometer Ultima3) at 298 K.

4. Evaluation of the photothermal sensitivity by NIR laser irradiation

Gold nanoplates solution (37.9 μg) were prepared in glass vials to investigate the photothermal effect induced by NIR laser irradiation. This solution was exposed to NIR coherent diode laser light (λ=808 nm, UM30K, Jenoptik) for 8 min, and the evaluation of

the solution temperature was monitored by a thermocouple (187 True RMS Multimeter, Fluke). As a control, deionized (DI) water was performed at same condition [28,29].

5. Biocompatibility tests

The biocompatibility of gold nanoplates against RAW264.7 cells as macrophage cells, which were obtained from the KOREAN CELL LINE BANK, was evaluated by measuring the inhibition of cell growth using MTT assay [23]. RAW264.7 cells were cultured in DMEM containing 10% FBS and 1% antibiotics at 37°C in a humidified atmosphere with 5% CO_2. First, these cells (2×10^4 cells /well) were seeded in 96-well plates the day before and incubated overnight. And then, various concentrations of gold nanoplates were treated in these cells. After 24 h, these cells were washed with PBS and performed the MTT assay. The relative percentage of the cell viability was calculated as the ratio of the absorbance in viable cells treated with gold nanoplates to the intensity in non-treated cells.

6. Cellular internalization

RAW 264.7 cells (2×10^5 cells /well) were seeded in 12-well plates the previous day and the incubated gold nanoplates in media without FBS for 12 h. Gold nanoplates-treated cells were washed three-times with PBS and harvested. Subsequently, after collection, the cells were fixed using the fixation and embedding protocols for resin section TEM and sectioned using a LEICA Ultracut UCT Ultramicrotome (Leica Microsystems). The cellular internalization of gold nanoplates was confirmed by TEM (JEOL-1100).

7. In vitro photothermal ablation study by NIR laser irradiation

Raw 264.7 cells (3×10^4 cells /well) were seeded in 96-well plate overnight and then treated with gold nanoplates (28.5 μM) in media without FBS for 18 h at 37°C. After incubation, the cells were rinsed with PBS and added serum free media. For the NIR laser irradiation experiment, the cells were exposed to a NIR coherent diode laser for 5 min at 20 W/cm^2. Then these cells were washed with PBS and further incubated for 4 h. We stained these cells using calcein AM (Molecular Probes) for 30 min to observe the distribution of the live cells by an optical system microscope (Olympus BX51).

III. Results and Discussion

Gold nanoplates were fabricated by the one-pot synthetic strategy. In this reaction, gold ions (Au^{3+}) were reduce to gold (Au^0) by pyrenyl dextran as a reducing agent and template, generating gold nanoplates as previously reported [Fig. 1(a)] [26]. Pyrenyl dextran form stable adlayers on gold surfaces and promote the growth of gold nanoplates by reducing gold ions to elemental gold [23-25]. Significantly, besides spherical shaped gold nanoparticles, other unique anisotropic gold nanomaterials have also been synthesized on pyrene-based materials, pyrenyl dextran. We analyzed gold nanoplates by scanning electron microscopy (SEM) and transmission electron microscopy (TEM) that they are formed several different shapes including large polygons, mainly hexagons, as well as small spheres [Fig. 1(b) and (c)]. In addition, when we observed them at the lower contrast, they were flat unlike the spherical nanoparticles around them. The X-ray diffraction (XRD) pattern of gold nanoplates were assigned to diffraction from the {111}, {200}, {220}, and {311} planes, corresponds to the well-known face centered cubic (fcc) facets of gold [Fig. 2(a)]. The polycrystalline natures of the gold nanoplates are revealed by electron diffraction patterns [Fig. 2(b)]. Based on these patterns, we an-

ticipated that pyrenyl dextran specifically bound to other facets of gold than {111} facets and its specific binding also served as reductant for growing gold (Au^{3+}) at the growing crystals. As gold nanopaltes grew, pyrenyl dextran bound onto face other than {111} facets thus increasing the area of the {111} facets. That is why gold nanoplates are mainly dominated by {111} facets [31,32].

The vis-NIR absorption spectrum obtained for gold nanoplates are shown in Fig. 2(c). They showed the characteristic surface plasmon resonance (SPR) band at 560 nm. As shown TEM images, small spherical gold nanoparticles are seen to coexist with hexagonally shaped gold nanoplates. In addition, they broadly absorbed in the NIR regions without maximum absorption peaks, which was assignable to the longitudinal surface plasmon absorption for hexagonal shaped gold nanoplates. This tendency was consistent with SEM and TEM images.

We also confirmed vis-NIR absorption of only pyrenyl dextran at the same concentrations in the absence of $HAuCl_4$ solution whether the optical property of pyrenyl dextran affects absorption patterns. It showed rarely absorption as we expected [Fig. 2(c)]. Thus, pyrene-templated hexagonal gold nanoplates exhibited absorption spectra with wide range, from visible to NIR regions, although gold nanoplates covered 52.5 wt% of pyrenyl dextran [Fig. 2(d)].

We next performed the cell viability of gold nanoplates against the macrophage (RAW 264.7) cells using MTT assay after incubation for 24 h. The gold nanoplates showed biocompatibility without any inhibitory effect on the growth and proliferation [Fig. 3(a)]. The large amount of gold nanoplates in the intracellular region exhibited without damaging the cellular structures, even at the high concentrations, indicating that they were efficiently internalized into the target cells (RAW 264.7 cells) by the strong interactions between gold nanoplates and scavenger

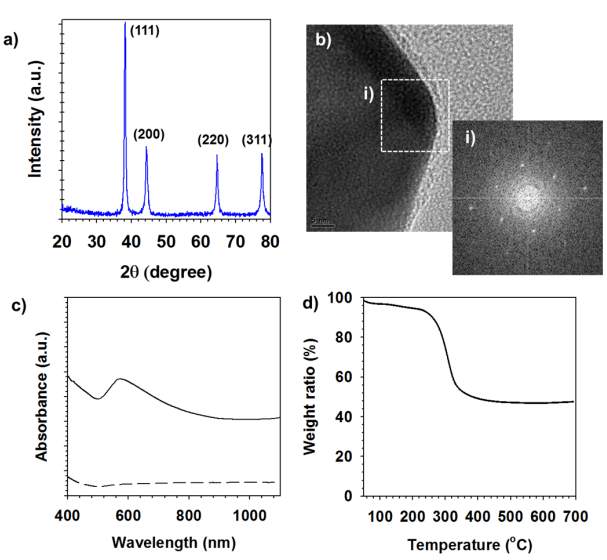

Figure 2. (a) X-rady diffraction (XRD) pattern of gold nanoplates, (b) HRTEM image shown its crystallinity (c) optical absorption spectrum (solid line: gold nanopaltes and dash line: pyrenyl dextran) and (d) thermogravimetric analysis of gold nanopaltes.

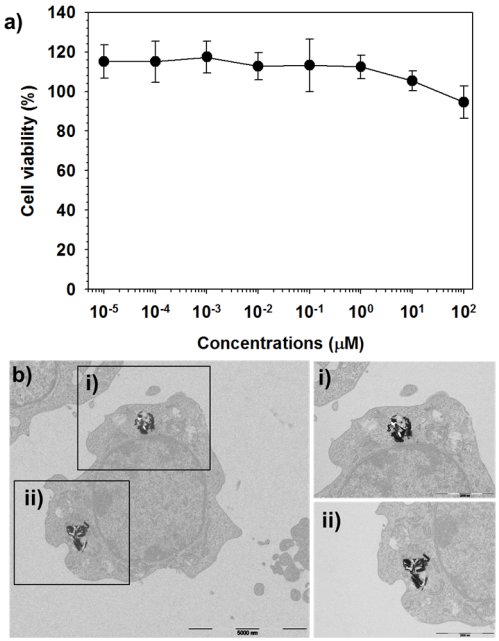

Figure 3. (a) Viability of RAW264.7 cells treated with various concentration of hexagonal shaped gold nameplates and (b) cross-sectional TEM images of RAW264.7 cells incubated with them (i and ii: high magnification).

receptors in the macrophages [Fig. 3(b)]. These gold nanoplates internalization within cells is a potentially important factor for effective localized photothermal treatment of cancer.

We estimated that gold nanoplates have the potentials to use as photothermal agents because they exhibited somewhat NIR absorption. Hence, we measured the temperature elevation rate of gold nanoplates solutions under NIR laser (λ=808 nm, 10 W/cm^2)) irradiation for 10 min. Absorbed light at the plasmon resonance frequency to gold nanoplates was converted into heat. This generated the photothermal heat increased temperature of the solution from 25°C to 42°C due to heat transfer from the gold nanoplates to the environment, while temperature of water as control was almost unchanged [Fig. 4(a)]. Especially, gold nanoplates containing solution generated heat more than only water which lead to increase in temperature by 16°C. On the basis of this result, we further evaluated *In vitro* phtothermal ablation potentials of gold nanoplates against macrophages upon NIR laser irradiation. The cells were incubated with the gold nanoplates (5.6 μg_{Au}/mL, 28.5 μM) for 24 h and each condition was irradiated by NIR laser for 5 min with a laser power density (20 W/cm^2). Afterward, calcein AM staining was conducted to distinguish the live/dead cells, which emits fluorescence after internalization into live cells as membrane-permeable green fluorescent cell marker. After NIR laser irradiation, gold nanoplates-treated cells only showed dark hole at laser-irradiated spot, indicating dead cells, whereas the other control groups were hardly damaged with showing strong green fluorescence [27,33]. Therefore, these results demonstrated the feasibility of gold nanoplates as photothermal therapy agents.

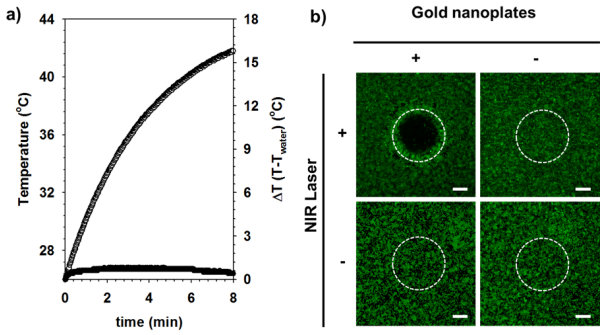

Figure 4. (a) Temperature profile for hexagonal-shaped gold nanoplates (white circle) and deionized water (black circle) irradiated by NIR laser (λ=808 nm, 10 W/cm^2). (b)Fluorescence microscopic images of RAW264.7 cells stained with calcein AM upon NIR laser irradiation (λ=808 nm, 20 W/cm^2) for 5min after treatment with gold nanoplates and only laser as a control. White circle indicates laser beam location (scalebar: 200 μm).

IV. Conclusions

We have developed hexagonal-shaped gold nanoplates by spontaneous reduction on pyrene-template molecules without additional reducing agents that this approach is of considerable interest and importance as it offers a facile method for synthesis of well-controlled gold nanoplates. Pyrene-modified polymer was selectively adsorbed on the plane of gold nanoplates and gold nanoplates have grew along {111} direction. The as-synthesized hexagonal shaped-gold nanoplates exhibited the near-infrared (NIR) absorption as well as biocompatibility. These properties support its use in potential capabilities for the phtothermal therapy of cancer. We anticipate that this method will be applied for synthesis of other noble metals, such as Pt, Pd, etc.

Acknowledgements

This study was supported by a grant from a National Research Foundation of Korea (NRF) grants funded by the Ministry of Education Science & Technology, Republic of Korea (2012-2043991).

References

[1] T. Soejima and N. Kimizuka, J. Am. Chem. Soc. **131,** 1447, (2009).

[2] A. M. Gobin, E. M. Watkins, E. Quevedo, A. L. Colvin, J. L. West, Small **6,** 745 (2010).

[3] J. E. Millstone, G. S. Métraux, and C. A. Mirkin, Adv. Funct. Mater. **16,** 1209, (2006).

[4] B. D. Busbee, S. O. Obare, and C. J. Murphy, Adv. Mater. **15,** 414, (2003).

[5] A. J. Frank, N. Cathcart, K. E. Maly, V. Kitaev, and J. Chem. Educ. **87,** 1098, (2010).

[6] X. Huang, S. Li, Y. Huang, S. Wu, X. Zhou, S. Li, C. L. Gan, F. Boey, C. A. Mirkin, and H. Zhang, Nat. Commun. 2:292, doi: 10.1038/ncomms1291 (2011).

[7] J. D. S. Newman and G. J. Blanchard, Langmuir **22,** 5882 (2006).

[8] N. G. Bastus, J. Comenge, and V. Puntes, Langmuir **27,** 11098 (2011).

[9] D. R. Bhumkar, H. M. Joshi, M. Sastry, and V. B. Pokharkar, Pharm. Res. **24,** 1415 (2007).

[10] Y. Gao, A. Voigt, M. Zhou, and K. Sundmacher, Eur. J. Inorg. Chem. **24,** 3769 (2008).

[11] N. Malikova, I. Pastoriza-Santos, M. Schierhorn, N. A. Kotov, and L. M. Liz-Marzán, Langmuir **18,** 3694 (2002)

[12] H. Yoo, J. E. Millstone, S. Li, J.-W. Jang, W. Wei, J. Wu, G. C. Schatz, and C. A. Mirkin, Nano. Lett. **9,** 3038 (2009).

[13] S. S. Shankar, A. Rai, B. Ankamwar, A. Singh, A. Ahmad, and M. Sastry. Nat. Mater. **3,** 482 (2004)

[14] Z. Guo, X. Fan, L. Liu, Z. Bian, C. Gu, Y. Zhang, N. Gu, D. Yang, and J. Zhang, J. Colloid. Interf. Sci. **348,** 29 (2010).

[15] S. P. Chandran, M. Chaudhary, R. Pasricha, A. Ahmad, and M. Sastry, Biotechnol. Prog. **22,** 577 (2006).

[16] S. S. Shankar, A. Rai, A. Ahmad, and M. Sastry, Chem. Mater. **17,** 566 (2005).

[17] Y. Sun, B. Mayers, and Y. Xia, Nano. Lett. **3,** 675 (2003).

[18] A. Leiva, C. Salidías, C. Quezada, A. Toro-Labbé, F. J. Espinoza-Beltrán, M. Urzúa, L. Gargallo, and D. Radic, Eur. Polym. J. **45,** 3035 (2009).

[19] T. H. Ha, H.-J. Koo, and B. H. Chung, J. Phys. Chem. C. **111,** 1123 (2007).

[20] C. Xue, G. S. Métraux, J. E. Millstone, and C. A. Mirkin, J. Am. Chem. Soc. **130,** 8337 (2008).

[21] J. Zhang, W. Li, Y. Cheng, X. Zhang, and S. Huang, H. Ma. Mater. Chem. Phys. **119,** 188 (2010).

[22] K. Hamamoto, H. Kawakita, K. Ohto, and K. Inoue, React. Funct. Polym. **69,** 694 (2009).

[23] X. Zhou, X. Huang, X. Qi, S. Wu, C. Xue, F. Y. C. Boey, Q. Yan, P. Chen, and H. Zhang, J. Phys. Chem. C. **113,** 10842 (2009).

[24] X. Huang, S. Li, S. Wu, Y. Huang, F. Boey, C. L. Gan, and H. Zhang, Adv. Mater. **24,** 979 (2012).

[25] C. Tan, X. Huang, and H. Zhang, Mater. Today **16,** 1369 (2013).

[26] E. K. Lim, E. Jang, J. Kim, T. Lee, E. Kim, H. S. Park, J. -S. Suh, Y.-M. Huh, and S. Haam, J. Mater. Chem. **22,** 17518 (2012).

[27] J. Choi, J. Yang, E. Jang, J.-S. Suh, Y. -M. Huh, K. Lee, and S. Haam, Anti-Cancer Agent Me **11,** 953 (2011).

[28] R. Choi, J. Yang, J. Choi, E. -K. Lim, E. Kim, J. -S. Suh, Y. -M. Huh, and S. Haam, Langmuir **26,** 17520, (2010).

[29] J. Choi, J. Yang, D. Bang, J. Park, J. -S. Suh, Y. -M. Huh, and S. Haam, Small **8,** 746 (2012).

[30] Y. Shao, Y. Jin, and S. Dong, Chem. Comm. **2004,** 1104 (2004).

[31] J. Gao, C. M. Bender, and C. J. Murphy, Langmuir **19,** 9065 (2003).

[32] Y. N. Tan, J. Y. Lee, and D. I. C. Wang, J. Phys. Chem. C. **112,** 5463 (2008).

[33] M. N. Rylander, Y. Feng, J. Bass, and K. R. Diller, Ann. N. Y. Acad. Sci. **1066,** 222 (2005).